Int J Adv Manuf Technol (2016) 87:789–799
DOI 10.1007/s00170-016-8467-x

ORIGINAL ARTICLE

An efficient five-axis machining method of centrifugal impeller based on regional milling

Hong-Zhou Fan[1] · **Guang Xi**[1] · **Wei Wang**[1] · **Yan-Long Cao**[2]

Received: 28 August 2015 / Accepted: 1 February 2016 / Published online: 27 February 2016

Abstract This paper presents an efficient five-axis machining method of centrifugal impeller based on regional milling. As the base of the machining method, geometry of the centrifugal impeller and blade surface is analyzed, and sub-machining regions are presented through the division of the double three-cubic d non-uniform rational B-spline (NURBS) surface. In rough milling, the cutter parameters, tool path interval, tool path curves, and the fixed tool axis vector are calculated by the novel algorithm based on regional milling; the biggest cutter and smaller tool path length are obtained. In finish milling, for the aerodynamic performance of the finished impeller, the tool path curves are modified and interlinked to make them uniform and orderly. A modified algorithm of the finish milling of the blade surface is proposed, and not only are the machining errors reduced; their reasonable distribution is also realized. Numerical simulation and a real test impeller are presented as the test of the proposed method.

Keywords Centrifugal impeller · Geometric modelling · Tool path planning · Regional milling · Tool axis vector

✉ Guang Xi
xiguang@mail.xjtu.edu.cn

[1] School of Energy and Power Engineering, Xi'an Jiaotong University, No. 28 Xianning West Road, Xi'an 710049, Shaanxi Province, People's Republic of China

[2] School of Mechanical Engineering, Zhejiang University, Hangzhou, People's Republic of China

1 Introduction

Five-axis numerical control (NC) machining has been used to manufacture turbine impeller, aerospace parts, ship bodies, cars, and dies/moulds for many years. Compared with the conventional three-axis machining, five-axis machining can manufacture the particularly complex parts which always have the complex geometry and are represented by parametric and free-form surfaces in very difficult conditions [1, 2]. However, the two added axes also make their control and tool path planning much more difficult. In addition, the stability of material removal deserved more and more attention about the impact on the life of tool and machine [3]. In recent years, more and more researchers have studied on five-axis machining such as local gouging prevention, global interference avoidance, tool path planning, and tool orientation optimization [4].

Centrifugal impeller is a very important, complex, and expensive part component in the compressor [5]. By the rotation of the impeller, the mechanical energy is converted into the pressure energy of the gas which passes through the impeller channel. The channel is restricted by the hub and a circle of blades. The blades are the most important parts of the centrifugal impeller: suitable blades can make centrifugal impeller to provide the perfect compressor performance, slight vibration, small noise, and low energy consumption [6].

For the NC machining of centrifugal impeller, efficiency is one of the most important research directions and precision is another. Focusing on the research directions above, many researchers have proposed a series of algorithms for tool path planning [7–10]. Gradually, flank milling becomes the particularly popular machining method of the centrifugal impeller. Compaed with point milling, flank milling can reduce the machining time required and give a smooth machining surface [11]. Chu et al. [12, 13] presented a novel tool path planning

for five-axis milling with developable surface approximation. The method can automatically generate an interference-free tool path for flank milling of the ruled surface; further research generated a spline-curve-constrained tool path which can produce minimized geometrical deviations on the machined surface and reduce the dimensionality in the solution space. Zhang et al. [14] proposed a tool path optimization for flank milling of ruled surfaces based on the distance function. The optimization could take great topics into account, such as post-processing, feed rate scheduling, machining dynamics, and so on. Zheng et al. [15] proposed a five-axis flank milling method of centrifugal impellers based on the cutter size optimization and interference-free tool path generation. Further, the material removal rate was increased and a stronger tool shank during flank milling was provided. Chen et al. [16] proposed tool path planning for five-axis flank milling of ruled surfaces in consideration of NC linear interpolation. The optimal tool path was computed by a global search scheme based on a dynamic programming. Further, with the wide application of difficult-to-cut materials in aerospace industry, for the more demanding requirements of integrated impeller machining due to the kinds of limitations such as cutting vibration, great cutting force, and short tool life, a meaningful attempt using CNC high-speed grinding of integrated impeller is presented to improve the milling precision of the integrated impeller [17]. In recent years, one of the new research thinkings of efficient machining is attended gradually: through the dividing of the target region,the sub-machining regions can integrally describe the whole machining region as becoming simpler and tool path planning becoming easier. In this respect, Chen et al. [18] proposed an integrated framework of tool path planning in five-axis machining of centrifugal impeller with split blades. The machining process was divided into four operations, and the framework provided several computer-aided manufacturing functions that enable automatic generation of quality tool path curves. Fan and Xi [19] presented an optimizing tool path generation for three-axis machining of sculpture impeller blade surface. Slighter curvature and more efficient calculations were achieved on the four sub-surfaces, and the adaptive tool-path generation algorithm was obtained. Further, Fan et al. [20] proposed a five-axis rough machining method for centrifugal impeller with free-form blades. Through the calculation of the approximate ruled blade and four sub-machining layers, the layered and efficient five-axis rough machining tool path curves were calculated.

Focusing on the efficiency for the five-axis machining of the centrifugal impeller, combining the advantages of flank machining and the sub-surface machining method, this paper presents an efficient five-axis machining method of centrifugal impeller based on regional milling. As the base of regional milling, the analysis of the centrifugal impeller is presented, and the division of the machining region of the centrifugal impeller channel is realized through the division of the double three-cubic non-uniform rational B-spline (NURBS) surface. In rough milling, the choice of the cutter, the calculation of tool path interval, the planning of tool path curves, and the classified calculation of the fixed tool axis vector are studied to achieve the efficient machining. In finish milling, the interlinking of the tool path curves on different regions and the optimizing of the tool interference are proposed to reduce the machining error and realize the reasonable distribution of the errors. Finally, the efficient five-axis machining method of centrifugal impeller based on regional milling is simulated and a real test impeller is machined.

2 Geometric modeling of the centrifugal impeller

Blade surface is the core part of the centrifugal impeller. Its geometric outline is restricted by four space curves, namely, shroud edge, hub edge, leading edge, and trailing edge. More specifically, the space points in the shroud edge and hub edge are the most important factors: shroud edge and hub edge are restricted by the space points; a series of lines which are restrained by the space points in the shroud edge and hub edge, respectively, are full of the blade surface; and the leading edge and trailing edge are the first line and last line of the lines above (Fig. 1a). The hub is another important part of the centrifugal impeller. It is mainly obtained through rotating the hub edge of the blade around the impeller axis. Figure 1b shows geometry of the centrifugal impeller, and it is composed of three parts: the hub, the blades, and the split blades. The hub is in the lower part of the centrifugal impeller; the blades and split blades are equally arranged around the impeller axis on the hub. Two adjacent blades, a split blade in the middle of the two blades, and a hub between the two blades, can comprise a channel. The channel is the target region for the five-axis machining of the centrifugal impeller; the whole impeller machining can be finished through the repetition of the channel machining by rotating the impeller. There are 11 channels in Fig. 1b.

Figure 2 shows a single channel of the centrifugal impeller in Fig. 1b. Further, it is restrained by five surfaces: hub, left blade pressure surface, split blade suction surface, split blade pressure surface, and right blade suction surface. For the traditional tool path planning methods, they always generate the tool path curves which pass through the whole channel. An inherent shortcoming of them is that the length of the tool path curves is too long. The lengthy tool path causes low machining efficiency. Another shortcoming is that the frequent change of the tool axis vector, which is calculated based on the molded lines of the blades as shown in Fig. 1a, can cause vibration. Unfortunately, the vibration can affect the machining precision and efficiency simultaneously.

Finding an efficient five-axis machining method to reduce the length of the tool path curves and diminish the change

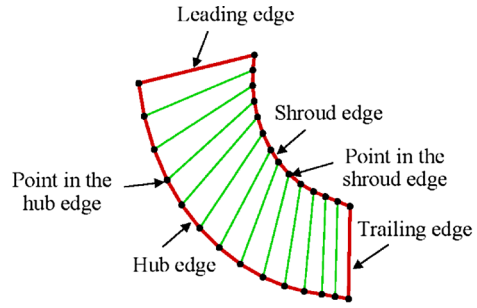

(a)

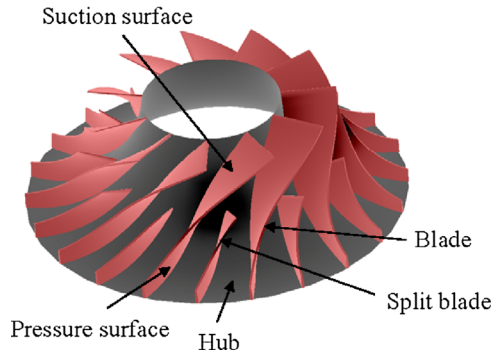

(b)

Fig. 1 Geometry of the ruled blade surface and centrifugal impeller. **a** Ruled blade surface. **b** Centrifugal impeller

frequency of the tool axis vector in the milling of the centrifugal impeller is the basic research idea of the paper. Regional milling is the research method to achieve the research idea. The division of the machining region of the centrifugal impeller channel is the first step of the method.

3 Division of the centrifugal impeller channel

All the space surfaces which compose the centrifugal impeller channel can be expressed as double three-cubic NURBS form in the matrix form as:

$$S(u,v)=\frac{UN_uP_wN_v^TV^T}{UN_uWN_v^TV^T}$$
$$(0\le u\le 1, 0\le v\le 1, i=1,2,\ldots,m, j=1,2,\ldots,n) \quad (1)$$

where v is the direction from shroud edge to hub edge, u is the direction from leading edge to tailing edge, N_u and $N_v{}^T$ are the primary function matrices, P_w is the characteristic point matrix, and W is the weighted factor matrix of P_w.

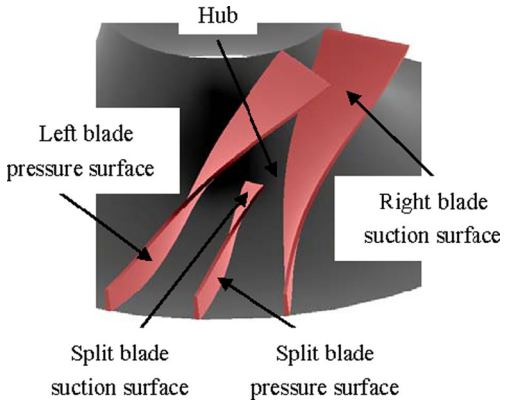

Fig. 2 Channel of the centrifugal impeller

$p_{(i,j)}$, U, V, W, X, Y, and Z are defined as:

$$p_{(i,j)}=\begin{bmatrix}x_{(i,j)}\\ y_{(i,j)}\\ z_{(i,j)}\end{bmatrix}\in P_W=\begin{bmatrix}X\\ Y\\ Z\end{bmatrix}\in R^3 \quad (2)$$

$$U=[u_0,u_1,\ldots,u_{m+4}]; \quad (3)$$

$$V=[v_0,v_1,\ldots,v_{n+4}]; \quad (4)$$

$$W=\begin{bmatrix}w_{(0,0)} & w_{(0,1)} & \cdots & w_{(0,n)}\\ w_{(1,0)} & w_{(1,1)} & \cdots & w_{(1,n)}\\ \vdots & \vdots & \ddots & \vdots\\ w_{(m,0)} & w_{(m,1)} & \cdots & w_{(m,n)}\end{bmatrix}; \quad (5)$$

$$X=\begin{bmatrix}w_{(0,0)}\cdot x_{(0,0)} & w_{(0,1)}\cdot x_{(0,1)} & \cdots & w_{(0,n)}\cdot x_{(0,n)}\\ w_{(1,0)}\cdot x_{(1,0)} & w_{(1,1)}\cdot x_{(1,1)} & \cdots & w_{(1,n)}\cdot x_{(1,n)}\\ \vdots & \vdots & \ddots & \vdots\\ w_{(m,0)}\cdot x_{(m,0)} & w_{(m,1)}\cdot x_{(m,1)} & \cdots & w_{(m,n)}\cdot x_{(m,n)}\end{bmatrix}; \quad (6)$$

$$Y=\begin{bmatrix}w_{(0,0)}\cdot y_{(0,0)} & w_{(0,1)}\cdot y_{(0,1)} & \cdots & w_{(0,n)}\cdot y_{(0,n)}\\ w_{(1,0)}\cdot y_{(1,0)} & w_{(1,1)}\cdot y_{(1,1)} & \cdots & w_{(1,n)}\cdot y_{(1,n)}\\ \vdots & \vdots & \ddots & \vdots\\ w_{(m,0)}\cdot y_{(m,0)} & w_{(m,1)}\cdot y_{(m,1)} & \cdots & w_{(m,n)}\cdot y_{(m,n)}\end{bmatrix}; \quad (7)$$

$$Z=\begin{bmatrix}w_{(0,0)}\cdot z_{(0,0)} & w_{(0,1)}\cdot z_{(0,1)} & \cdots & w_{(0,n)}\cdot z_{(0,n)}\\ w_{(1,0)}\cdot z_{(1,0)} & w_{(1,1)}\cdot z_{(1,1)} & \cdots & w_{(1,n)}\cdot z_{(1,n)}\\ \vdots & \vdots & \ddots & \vdots\\ w_{(m,0)}\cdot z_{(m,0)} & w_{(m,1)}\cdot z_{(m,1)} & \cdots & w_{(m,n)}\cdot z_{(m,n)}\end{bmatrix}. \quad (8)$$

For the target ruled blade surface, its double three-cubic NURBS form can be rewritten as:

$$S(u,v)=vC_{i,n}(u)+(1-v)C_{i,n}(u); \quad (9)$$
$$(0\le u\le 1, 0\le v\le 1, i=1,2,\ldots,m)$$

where $C_{i,1}(u)$ and $C_{i,n}(u)$ are the baselines of the ruled blade surface; n flow lines are from shroud edge to hub edge and m points are in each flow line. Obviously, $C_{i,1}(u)$ and $C_{i,n}(u)$ are the first and last flow lines in the ruled blade surface, respectively, as shown in Fig. 3.

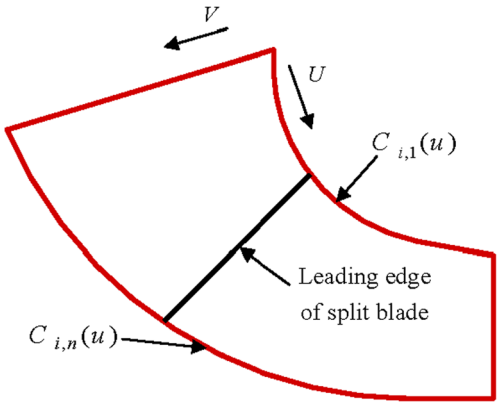

Fig. 3 NURBS surface of the ruled blade

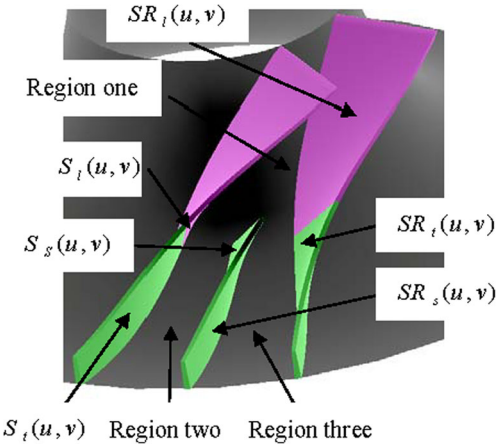

Fig. 4 Sub-regions of the centrifugal impeller channel

The split blade is part of the blade in geometry and is located in the middle between the two adjacent blades. As shown in Figs. 2 and 3, from inlet to outlet, the channel is divided into three sub-regions and the leading edge of the split blade is the intersecting line of the three sub-regions above.

$k \in (1, m)$ is defined as the location of the leading edge of the split blade in the shroud edge of the blade; the split blade can be expressed as:

$$S_s(u,v) = vC_{s,i,1}(u) + (1-v)C_{s,i,n}(u); \quad (10)$$

$$(0 \le u \le 1, 0 \le v \le 1, i = k, k+1, \ldots, m)$$

Then, the blade surface can also be split into two sub surfaces. $S_l(u,v)$ and $S_t(u,v)$ are defined as the sub-surfaces near the leading edge and trailing edge, respectively. So, there are

$$S_l(u,v) = vC_{l,i,1}(u) + (1-v)C_{l,i,n}(u); \quad (11)$$

$$(0 \le u \le 1, 0 \le v \le 1, i = 1, 2, \ldots, k)$$

$$S_t(u,v) = vC_{l,i,1}(u) + (1-v)C_{l,i,n}(u); \quad (12)$$

$$(0 \le u \le 1, 0 \le v \le 1, i = k, k+1, \ldots, m)$$

Therefore, three sub-regions are constrained through the surfaces above. As shown in Fig. 4, region one is between two sub-surfaces near the leading edge, where $S_l(u,v)$ is on the left and $SR_l(u,v)$ is on the right; region two is between two sub-surfaces of $S_t(u,v)$ and $S_s(u,v)$ near the trailing edge; and region three is between two sub-surfaces of $SR_s(u,v)$ and $SR_t(u,v)$ near the trailing edge.

4 Tool path planning of rough milling

In rough milling, facing the target part which still is a solid blank, the main purpose is to remove the needleless material between each pair of adjacent blades (split blades) as quickly as possible. In theory, choosing the biggest cutter and the shortest tool path length is the direct research idea. A novel and efficient method is attempted in this research. Region one in Fig. 4 is the first research focus.

In particular, tool path planning of rough milling is a complex calculation, which constituted the choice of the biggest cutter, calculation of the tool path interval, tool path planning, and calculation of the fixed tool axis vector.

4.1 Choice of the biggest cutter

The value of the cutter diameter must be calculated firstly. For region one in Fig. 4, the machining region is restrained by $S_l(u,v)$, $SR_l(u,v)$, and a part of the hub. p_l is defined as every point in $S_l(u,v)$, p_{rl} is defined as every point in $SR_l(u,v)$, and d_{l1} is defined as the distance between the points in $S_l(u,v)$ and $SR_l(u,v)$ respectively, so there is

$$d_{l1} = |p_l - p_{rl}| \quad (13)$$

$MINd_1$ is defined as the minimum range of the cutter which can pass through the channel, and it can be calculated as:

$$MINd_1 = \min(d_{l1}) \quad (14)$$

D_1 is defined as the maximum diameter of the cutter, and it would be restrained by the Boolean relation as:

$$D_1 \le MINd_1 \quad (15)$$

Obviously, $D_1 = [MINd_1]$ is the biggest value of the cutter diameter.

The tool geometry is another important technological parameter in the choice of the cutter. For the traditional machining, ball-end cutter and flat-end cutter are two common cutters to mill the complex parts. Keeping the advantages of the two types of cutters, the easiness of the tool path planning using ball-end cutter machining and the high efficiency of the real milling using flat-end cutter machining, a type of cutter named bull-nose-end cutter is used in this research.

4.2 Calculation of the tool path interval

Rough milling is a process that uses the cutter to remove most of the unused material of the impeller. Tool path interval is the determiner to get the number of tool path curves and the tool path length.

As shown in Fig. 5a, the tool path interval is determined by the radius of the ball-end cutter and the given scallop height along a pair of adjacent tool path curves. The actual target surface is approximated by a circular arc with a radius of curvature ρ ($\rho<0$ for a concave surface and $\rho>0$ for a convexity surface) ordinarily. L is defined as the tool path interval and it can be calculated by [21]:

$$L = 2\sqrt{2{\cdot}r{\cdot}h - h^2} \tag{16}$$

Then, for the scallop which is formed by the contour of the cutter, the intersecting plane interval δ is calculated by:

$$\delta = L\cos\theta = 2\sqrt{2{\cdot}r{\cdot}h - h^2}{\cdot}\cos\theta \tag{17}$$

The quite other scallop is shown in Fig. 5b using the bull-nose-end cutter: a sequence of flat and sharp cusps generated over the surface [22], the scallop is the combination of the scallops which is determined by the ball-end cutter and the flat-end cutter separately. With the same scallop height, the tool path interval using the bull-nose-end cutter is wider than that using the ball-end cutter. Further, because the flat cusps are lower than the sharp cusps in the whole process, the calculation of the tool path interval can overlook the flat cusps. So, it is similar to that using the ball-end cutter. In conclusion, the calculation of the tool path interval is efficient and concise. Compared to Fig. 5a, the straight-line segment radius d is added as shown in Fig. 5b. The tool path interval with bull-nose-end-mill L' is then calculated by:

$$L' = 2\sqrt{2{\cdot}r{\cdot}h - h^2} + d \tag{18}$$

Accordingly, the intersecting plane interval with bull-nose-end cutter δ' is then calculated by:

$$\delta' = L\cos\theta = \left(2\sqrt{2{\cdot}r{\cdot}h - h^2} + d\right){\cdot}\cos\theta \tag{19}$$

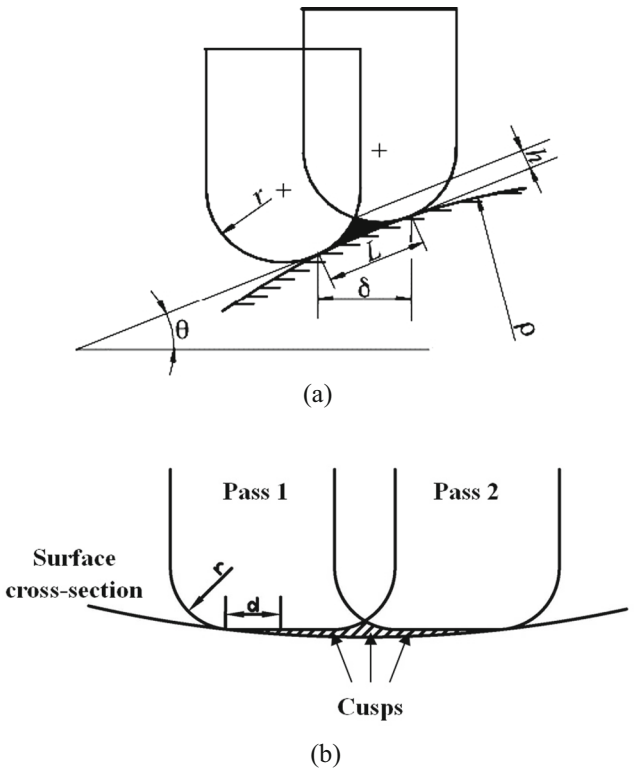

Fig. 5 Scallop height and tool path interval. **a** Tool path interval of the ball-end cutter. **b** Tool path interval of the bull-nose-end cutter

4.3 Tool path planning

After the choice of the cutter and the calculation of the tool path interval, the mathematical basis is basically ready for the tool path planning. For the efficient and orderly tool path curves, tool path planning is the important technology process subsequently. Tool path planning in this research is described as follows:

1. Define $C_{l,i,n}(u)$ and $CR_{l,i,n}(u)$ as the basal lines of the algorithm. They are the baselines of the ruled blade surfaces $S_l(u, v)$ and $SR_l(u, v)$, as well as the intersecting curves of the blade surfaces above and the hub.
2. According to the intersecting plane interval with bull-nose-end cutter δ', $C_{l,i,n}(u)$ and $CR_{l,i,n}(u)$ move δ' from their original position to the middle of the channel, and the first batch tool path curves in the hub are obtained.
3. Calculate the distance of the end points in the new tool path curves.
4. If the distance is lesser than the diameter of the bull-nose-end cutter, the algorithm would be finished.
5. If the distance is greater than the diameter of the bull-nose-end cutter, the calculation goes to step 6.
6. Calculate the intersecting point of the two tool path curves which is obtained in step 2 above.
7. If the intersecting point does not exist, $C_{l,i,n}(u)$ and $CR_{l,i,n}(u)$ are replaced by the first batch of tool path curves obtained in step 2. The moving of the curves in step 2 proceeds and the next-batch tool path curves in the hub are obtained.
8. If the intersecting point exists, cut off the two tool path curves in the intersecting point and remove the parts of the two tool path curves near the inlet. So, $C_{l,i,n}(u)$ and $CR_{l,i,n}(u)$ are replaced by the shorter curves. The moving of the new curves in step 2 proceeds and the next-batch tool path curves in the hub are obtained.

9. Repeat the calculation from step 2 to step 8, where all the tool path curves would be obtained.

Figure 6 is the sketch of the tool path planning; the tool path curves are obtained from $C_{l,i,n}(u)$ and $CR_{l,i,n}(u)$ to the middle of the channel in pairs. The first-batch tool path curves near the blade surfaces are the longest. The nearer that tool path curves approximate to the middle, the shorter their lengths are.

One thing to note is the starting points of the shorter curves. For the tool path planning of the traditional machining which mills the channel from inlet to outlet, the starting points and the end points are out of the channel; the approach and escape motions are free of interference. The difference is that the starting points of this tool path planning are in the channel and the approach motion requires special care. The dotted line in the middle is the added curves from the inlet of the channel to every intersecting point (starting point) of the shorter curves; it proposes the free location for the approach motion.

4.4 The fixed tool axis vector

In five-axis NC machining of the complex parts, the tool axis vectors are changing constantly. The changing tool axis vectors can pass through the warping interspaces and surfaces; however, its inherent disadvantage is inefficiency. In rough milling, the main purpose is to remove the needleless material in the channel as quickly as possible. That is to say, the primary purpose in this process is not precision, but efficiency. For the stability of NC machining, compared with the three-axis machine, the five-axis machine has weaker structural and dynamic characteristics. So, keeping the tool axes of the machine relatively stable is a promising thought, and fixing the tool axis vector is an effective machining method. For the tool path curves in the channel (as shown in Fig. 6), two different strategies are proposed purposefully.

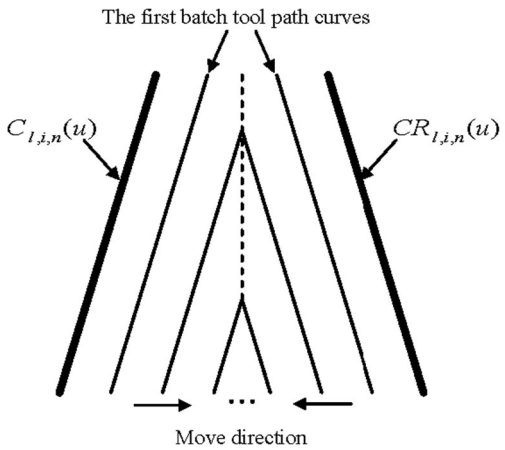

Fig. 6 Tool path planning

The first strategy focuses on the first-batch tool path curves in the hub. Because of the interference of the blade surfaces, the tool axis vectors of the tool path curves must keep the similar changing with the space lines which are restricted by shroud edges and hub edges of $S_l(u, v)$ and $SR_l(u, v)$, respectively. Another strategy focuses on the other tool path curves except the first batch. Because the tool path curves are relatively far from the blade surface, the interference is not a key problem which must be paid critical attention to. Fixing the fixing tool axis vector to increase the machining efficiency is then the primary purpose at this stage. Near the inlet, the workspace is wide enough for the calculation of the tool axis vectors. So, the research workspace of this strategy focuses on the zone near the outlet of region one. At the same time, the split blade is in there to increase the difficulty of the tool movement. For these reasons, defining the space vectors of the leading edge of the split blade as the fixed tool axis vectors is the optimal decision.

The whole tool axis vector calculation can be described as follows:

1. Classify the tool path curves as two types: the first-batch tool path curves and the others.
2. For the tool path curves which belong to the first batch, the space vectors of the space lines are defined as the tool axis vectors of the tool path curves. Go to step 8.
3. For the tool path curves which do not belong to the first batch, calculate the space vector of the leading edge of the split blade.
4. Define the space vector which is calculated in step 3 as the tool axis vectors of all the cutting contact points in all the tool path curves.
5. Introduce the tool parameters; simulate the real cutting in the channel.
6. If the cutting is interference-free, go to step 8.
7. If the cutting is interferential, modify each interferential tool axis vector to avoid interference; change the two adjacent tool axis vectors (before and after each interferential tool axis vector) to smoothen the tool path.
8. Synthesize all the tool axis vectors and finish the calculation.

Through the calculation from sections 4.1 to 4.4 above, a novel and efficient tool path planning method of rough milling for region one is presented. For region two or region three, from sections 4.1 to 4.3, the tool path planning method is the same as for region one; the difference is in the calculation of the fixed tool axis vector. In region two or region three, the fixed tool axis vector can tilt an angle.

Figure 7 shows two different types of fixed tool path vectors in different regions. α is the inclination angle from the tool axis vector in region one to the tool axis vector in region two or region three. Then, the milling becomes more efficient and smoother. Further, because of the added α, the tool axis

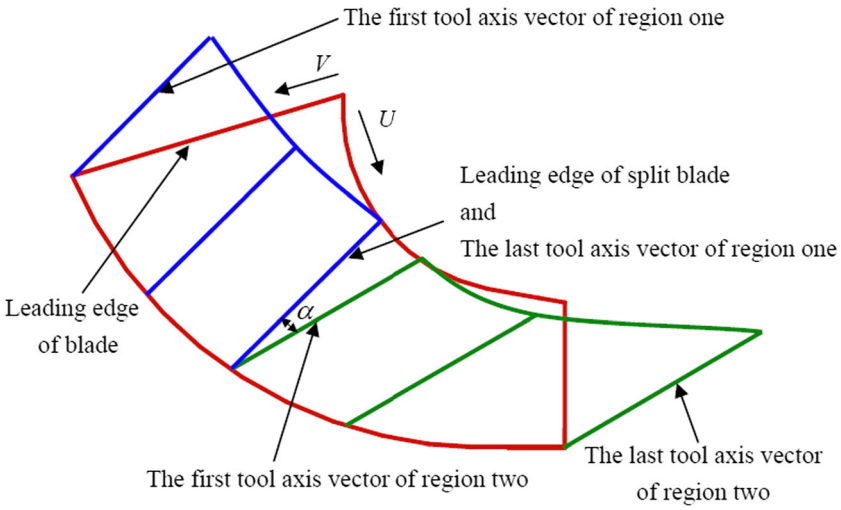

Fig. 7 The sketch of different fixed tool path vectors

vector in region two (or region three) is inclined from leading edge to trailing edge. If there are several interferential tool axis vectors which need to be modified, in the direction of rotation, the range of the controllable tilt angle can be modified to calculate the fixed tool path vectors, and interference avoiding becomes easier.

5 Tool path planning of finish milling

In finish milling, facing the target part which has removed most of the needleless metal material, the main purpose is to finish the surfaces of blades, split blades, and hub precisely. Except for the high efficiency which can be calculated through the method in step 4 above, some more in-depth technological requirements need to be met. The interlinking of the tool path curves on the different regions and the finish milling of the blade surfaces are two research emphases and difficulties which must be resolved.

5.1 Interlinking of the tool path curves on different regions

In rough milling, the cutter and the tool path curves are relatively uniform. By the method in sections 4.1 and 4.2, with the same accepted error, the cutter and the tool path interval in region one are bigger than those in the other regions. Accordingly, the tool path curves in region one are sparser than those in the other regions as well. In other words, the tool path curves are not consecutive from inlet to outlet in the whole channel. Figure 8 shows the inconsecutive tool path curves in different regions. It is advantageous for the machining efficiency, but disadvantageous for the aerodynamic performance of the finished impeller. So, the uniform cutter and orderly tool path curves are obligatory.

The interlinking method of the tool path curves on different regions is described as follows.

1. Take the curves of the outlet of region one as the base curve, and confirm the accepted Scallop height in finish milling.
2. Choose the ball-end cutter in the whole channel and calculate the tool path interval in the base curve using Eq. 18.
3. Calculate the cutter contact points in the base curves from the adjacent blades ($S_I(u, v)$ and $SR_I(u, v)$) to the middle of region one.
4. Calculate the tool path curves from outlet to inlet on region one (using the tool path planning method in section 4.3).
5. Calculate the first-batch tool path curves on region two and region three.
6. Calculate the tool path curves between the first-batch tool path curves on region two and region three (using the tool path planning method in section 4.3).
7. Create the relatively smooth transition adopting a circular arc.

Figure 9 shows the interlinking of the tool path curves on different regions. After optimizing and adjusting, the tool path curves become uniform and orderly.

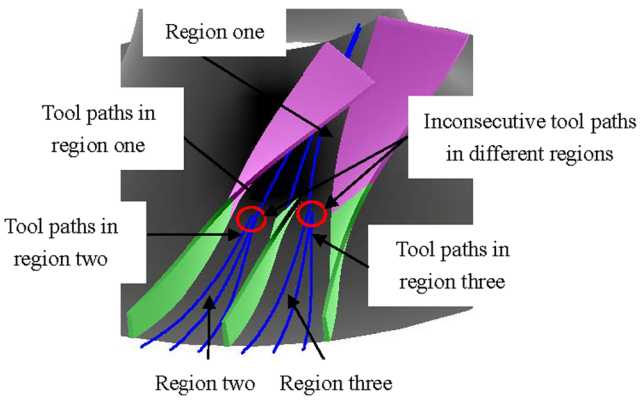

Fig. 8 Inconsecutive tool path curves in different regions

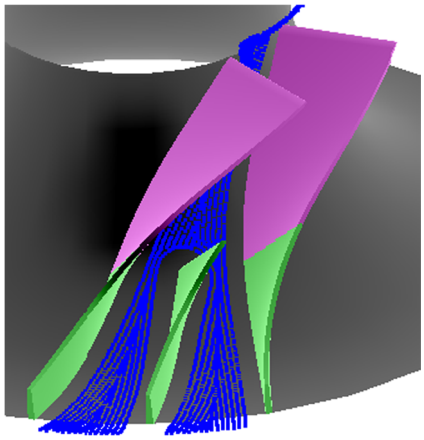

Fig. 9 Interlinking of the tool path curves on different regions

5.2 Finish milling of the blade surface

After rough milling, the target impeller blade is unshaped and needs to be milled further. The precision of the blade surface becomes the main purpose in this process. Of course, the tool axis vectors which were just calculated by the space vectors of the space lines could hardly meet the demands in machining precision.

For the flank milling of the ruled blade surface, the inherent problem is that the ruled blade surface is a non-developable surface, but the working envelope of the rotary cutter is a developable surface; the tool interference is inevitable. Figure 10 shows the tool interference occurring in flank milling of the ruled surface [12]. $C_{i,1}(u)$ and $C_{i,n}(u)$ are the shroud edge and hub edge of the ruled surface, respectively; the circle is the cutter and $D_1/2$ is the radius which is calculated in section 4.1; the cutter contacts a point in $C_{i,1}(u)$ and the tool axis is parallel to the ruled surface; and $C'_{i,1}(u)$ and $C'_{i,n}(u)$ are tangent vectors at the contact point of $C_{i,1}(u)$ and $C_{i,n}(u)$, respectively. Generally, $C'_{i,1}(u)$ and $C'_{i,n}(u)$ do not lie on the same plane with the ruled surface. So, the tool interference takes place around the contact point. Further, the cutter becomes tangent which is only fit to one curve $C_{i,1}(u)$ and the greatest amount of the overcut occurs near another curve $C_{i,n}(u)$. If β is defined as the angle extended by $C'_{i,1}(u)$ and $C'_{i,n}(u)$, the maximal overcut is $D_1(1-\cos\beta)/2$.

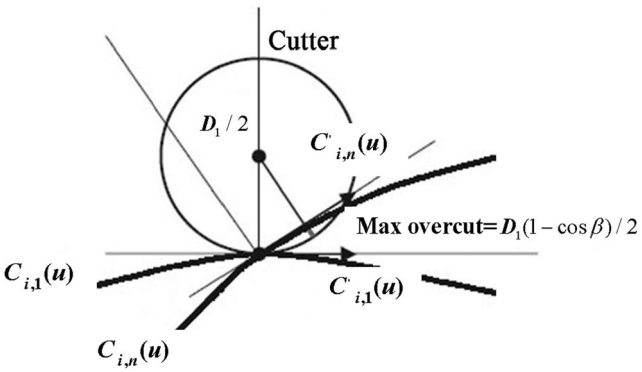

Fig. 10 Tool interference occurs in flank milling

Reducing the radius of the cutter can reduce tool interference, but that is negative for the efficient machining. Bohez et al. [23] explained that the overcut could be reduced by changing the relative position of the cutter and surface. So, the solution to reduce tool interference of the ruled blade surface milling can be described as follows.

1. Define shroud edge $C_{i,1}(u)$ and hub edge $C_{i,n}(u)$ as the ruling curves of the ruled surface.
2. Define $\Delta\theta$ as the acceptable error.
3. Extract the space curve $C_{i,(1+n)/2}(u)$ in the middle of the blade surface $S(u, v)$ as the base curve.
4. Define θ' as the angle extended by $C'_{i,1}(u)$ and the tangent vector $C'_{i,(1+n)/2}(u)$.
5. Define ε as the acceptable error.
6. Compare ε with $\theta/2$ (θ is the angle extended by $C_{i,1}(u)$ and $C_{i,n}(u)$).
7. If $|\theta'-\theta/2|\leq\varepsilon$, go to step 9.
8. If $|\theta'-\theta/2|>\varepsilon$, move the base curve $C_{i,(1+n)/2}(u)$ up or down; if $C_{i,(1+n)/2}(u)$ is replaced by $C_{i,((1+n)/2)-1}(u)$ or $C_{i,((1+n)/2)+1}(u)$, go to step 4.
9. Calculate the maximal overcut by $r(1-\cos(\theta/2))$.

Through the method above, comparing with the greatest amounts of the overcut, the tool interference is reduced obviously. Another advantage that this method can propose is the uniformity of the error distribution. The difference from Fig. 10 is as follows: near the middle of the blade surface, the error is the minimum value which can almost be regarded as zero; near the shroud edge and hub edge of the ruled surface, the errors are the biggest. The amount of the overcut and the gradient of the error distribution all become smaller. Figure 11 is the sketch of the finish milling of a pressure surface which is split into $S_l(u, v)$ and $S_r(u, v)$. By the tool path curves interlinking above, the finish milling of the pressure surface is passing through the whole channel.

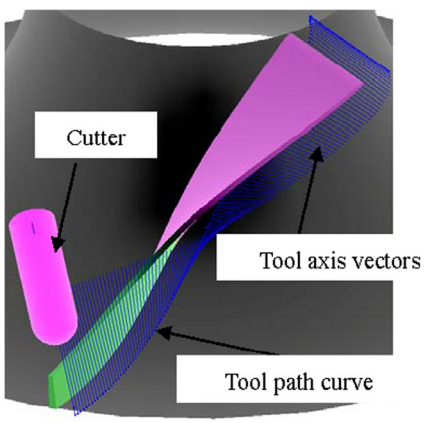

Fig. 11 Finish milling of pressure surface

6 Simulation and machining experiment

A test impeller with 11 blades and 11 split blades is provided to verify the five-axis efficient machining method: The diameter is 192 mm; the minimum width at which the cutter can pass through the channel is 10.759 mm.

Figure 12a shows the Cincinnati Milacron H5 horizontal machining center with Acramatic A950MC computer numerical control; it is chosen to machine the test impeller. For the machine tool, *X*, *Y*, and *Z* axes are the three translation axes; *A* and *B* axes are the two rotation axes. Further, as shown in Fig. 12b, *X* axis is the column axis; *Y* axis is the spindle carrier axis; *Z* axis is the pallet slide axis; *A* axis is the tilting spindle axis around *X* axis, and *B* axis is the rotary contouring pallet axis around *Y* axis. The maximum spindle speed is 3000 rpm,

(a)

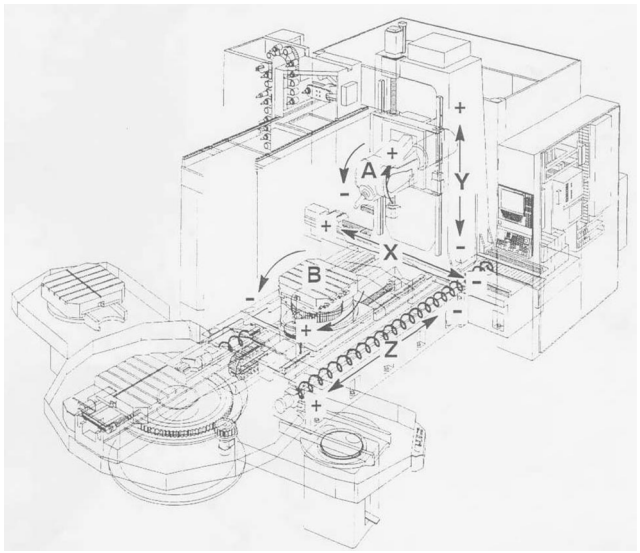

(b)

Fig. 12 Machine tool and its axis orientation. **a** Cincinnati Milacron H5 horizontal machining center. **b** Axis orientation of the Cincinnati Milacron H5 horizontal machining center

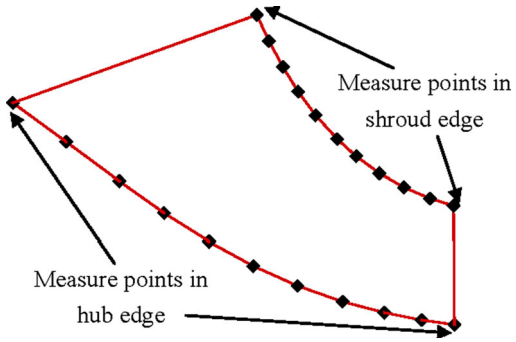

(a)

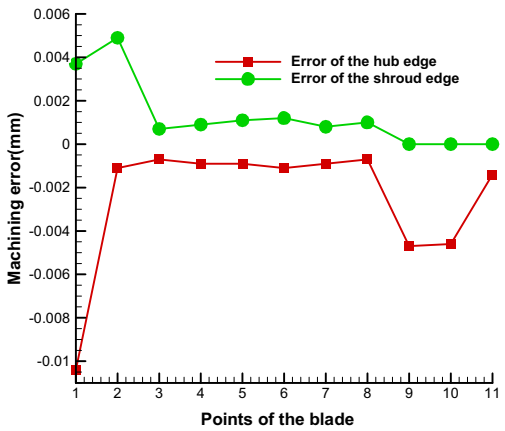

(b)

Fig. 13 Measure points and the machining error distribution in the pressure surface. **a** Measure point distribution in the pressure surface. **b** The machining error distribution in the pressure surface

and the cutter is calculated in section 4.1. The impeller is machined by the five-axis motion which is controlled by the tool path curves calculated above.

In rough milling, through the division of the machining region of the channel, two different minimum widths are obtained. In region one, the value is 12.952 mm; in the other regions, the values all are 10.759 mm. So, two different cutters (the diameters are 12 and 10 mm) are obtained to replace the

Fig. 14 The finished impeller

only cutter whose diameter is 10 mm. Then, in region one, the bigger cutter is chosen, and the shorter tool path length and higher feed rate are figured out to realize the efficient milling; in region two and region three, compared with the whole channel, the height of the cutting area becomes smaller (from 27.995 to 18.034 mm) and the needleless tool path curves are greatly decreased. Further, keeping the fixed tool axis vector in milling could be enormously beneficial to increase the feed rate and stability of the machine.

In finish milling, the whole finish milling includes the finish milling of the hub and the finish milling of blades. With the same appointed scallop height 0.035 mm and ball-end cutter (the diameter is 10 mm), for the finish milling of the hub, using the traditional machining method, the length of the tool path curves of impeller channel is 8650.48 mm; using the machining method in this research, the length of the tool path curves of impeller channel as shown in Fig. 9 is 6514.94 mm. About 25 % tool path length and milling time are saved obviously. For the finish milling of the blade surfaces, the blades are finished through the finish milling method as shown in Fig. 11. The tool path curves are passing through the whole channel from inlet to outlet of the blade surfaces. Figure 13a shows the distribution of the marked measure points in the pressure surface above. There are 11 measure points in the shroud edge and 11 measure points in the hub edge. For each measure point, the measurement of the machining error between the machined surface and the designed surface is taken. Figure 13b displays the distribution of the machining error by the lines and symbols. The result is same as the calculation in section 5.2, and the other blades have similar distribution of the machining error.

The efficient five-axis machining method of the centrifugal impeller is proved through the calculation and simulation above. Further, the test impeller is real milled and the finished impeller is shown in Fig. 14.

7 Conclusions

In this paper, an efficient five-axis machining method of centrifugal impeller based on regional milling is proposed. The analysis of the centrifugal impeller with split blades and the division of the machining region are presented to build the base of regional milling; in rough milling, a novel algorithm including the choice of the cutter, the calculation of scallop height and tool path interval, the planning of tool path curves, and the classified calculation of the fixed tool axis vector is proposed to decrease the tool path length and increase the feed rate; in finish milling, the interlinking of the tool path curves on different regions is obtained to satisfy the aerodynamic performance, and the new algorithm of the finish milling about the blade surface is proposed to reduce the machining error and realize the reasonable distribution of the errors.

The five-axis machining method can make the milling of centrifugal impeller with split blades more efficient and unhindered. The most direct advantage is the efficiency of saving machining time and costs. In the next step, the method needed to be more perfect and applied in the machining of the complex parts more broadly.

Acknowledgments The authors acknowledge the financial support provided by the National Basic Research Program (973 Program) of China (Grant No. 2011CB706505).

References

1. Young HT, Chuang LC, Gerschwiler K, Kamps S (2004) A five-axis rough machining approach for a centrifugal impeller. Int J Adv Manuf Technol 23(3–4):233–239
2. Fan JH, Ball A (2011) Integrated method for tool path generation in five-axis sculptured surface machining. Int J Prod Res 49(22): 6813–6831
3. He Y, Chen ZT, Xu RF, Wu XZ (2015) Reducing fluctuation of machining strip width by tool position modification for five-axis NC machining of sculptured surfaces. Int J Adv Manuf Technol 78(1):249–257
4. Wang N, Tang K (2008) Five-axis tool path generation for a flat-end tool based on iso-conic partitioning. Comput Aided Des 40(12): 1067–1079
5. Chen KH (2011) Investigation of tool orientation for milling blade of impeller in five-axis machining. Int J Adv Manuf Technol 52(1–4): 235–244
6. Wu CH (1952) A general theory of three-dimensional flow in subsonic and supersonic turbomachines of axial, radial, and mixed-flow types. NACA Technical Note 2604
7. Morishige K, Takeuchi Y (1997) 5-Axis control rough cutting of an impeller with efficiency and accuracy. Proceedings of the 1997 I.E. international conference on robotics and automation, pp 1241–1246
8. Chaves-Jacob J, Poulachon G, Duc E (2012) Optimal strategy for finishing impeller blades using 5-axis machining. Int J Adv Manuf Technol 58(5–8):573–583
9. Wu BH, Zhang DH, Luo M, Zhang Y (2013) Collision and interference correction for impeller machining with non-orthogonal four-axis machine tool. Int J Adv Manuf Technol 68(1–4):693–700
10. Han FY, Zhang DH, Luo M, Wu BH (2015) An approach to optimize the tilt angle of indexable table for nonorthogonal four-axis milling of impeller. Int J Adv Manuf Technol 76(9–12):1893–1904
11. Wu CY (1995) Arbitrary surface flank milling of fan, compressor, and impeller blades. Trans ASME J Eng Gas Turb Power 117(3): 534–539
12. Chu CH, Chen JT (2006) Tool path planning for five-axis flank milling with developable surface approximation. Int J Adv Manuf Technol 29(7–8):707–713
13. Chu CH, Hsieh HT, Lee CH, Yan CY (2015) Spline-constrained tool-path planning in five-axis flank machining of ruled surfaces. Int J Adv Manuf Technol 80(9):2097–2104
14. Zhang XM, Zhu LM, Zheng G, Ding H (2010) Tool path optimisation for flank milling ruled surface based on the distance function. Int J Prod Res 48(14):4233–4251
15. Zheng G, Zhu LM, Bi QZ (2012) Cutter size optimisation and interference-free tool path generation for five-axis flank milling of centrifugal impellers. Int J Prod Res 50(23):6667–6678
16. Chen CH, Wu PH, Li YW (2012) Tool path planning for 5-axis flank milling of ruled surfaces considering CNC linear interpolation. J Intell Manuf 23(3):471–480

17. Li X, Meng FJ, Cui W, Ma S (2015) The CNC grinding of integrated impeller with electroplated CBN wheel. Int J Adv Manuf Technol 79(5):1353–1361
18. Chen CH, Huang WN, Li YW (2012) An integrated framework of tool path planning in 5-axis machining of centrifugal impeller with split blades. J Intell Manuf 23(3):687–698
19. Fan HZ, Xi G (2012) Optimizing tool path generation for three-axis machining of sculpture impeller blade surface. Proc IMechE B J Eng Manuf 226(1):43–51
20. Fan HZ, Wang W, Xi G (2013) A novel five-axis rough machining method for efficient manufacturing of centrifugal impeller with free-form blades. Int J Adv Manuf Technol 68(5–8):1219–1229
21. Ding S, Mannan MA, Poo AN, Yang DCH, Han Z (2003) Adaptive iso-planar tool path generation for machining of free-form surfaces. Comput Aided Des 35(2):141–153
22. Gray PJ, Bedi S, Ismail F (2005) Arc-intersect method for 5-axis tool positioning. Comput Aided Des 37(7):663–674
23. Bohez ELJ, Senadheraet SDR, Pole K, Duflou JR, Tar T (1997) A geometric modeling and five-axis machining algorithm for centrifugal impellers. J Manuf Syst 16(6):422–436